# Polymer Chemistry

Accepted Manuscript

ROYAL SOCIETY OF CHEMISTRY

www.rsc.org/polymers

Magnetic polyaniline hollow spheres with the functionality of lead uptake were fabricated by using citric acid to decorate ferroferric oxide.

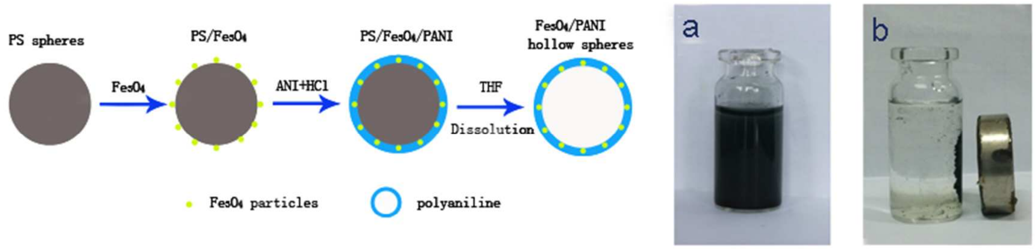

Cite this: DOI: 10.1039/c0xx00000x

www.rsc.org/xxxxxx

ARTICLE TYPE

# Fabrication of well-defined electromagnetic $Fe_3O_4$/polyaniline hollow microspheres and their application on $Pb^{2+}$ uptake†

**Feng Wang,[a] Liyan Huang,*[a] Jun Li,[a] Lina Lin,[a] Zhengping Liu[a] and Zhaoxia Dong[b]**

***Received (in XXX, XXX) XthXXXXXXXXX 20XX, Accepted Xth XXXXXXXXX 20XX***

**DOI: 10.1039/b000000x**

The well-defined superparamagnetic and conductive $Fe_3O_4$/polyaniline(PANI) hollow spheres were fabricated using positively charged polystyrene (PS) spheres as templates. The negatively charged $Fe_3O_4$ particles, which were decorated by citric acid, can be attached onto the surface of the PS spheres via electrostatic interaction. Subsequently, PANI layer was coated onto the PS/$Fe_3O_4$templates by in-situ chemical oxidative polymerization. Finally, removal of the PS core by dissolving with tetrahydrofuran provided the electromagnetic hollow spheres. Morphologies and compositions of $Fe_3O_4$/PANI hollow spheres were investigated by using SEM, TEM, FTIR and XRD. The magnetic analysis demonstrates that the synthesized composite spheres possess the characteristic of superparamagnetism and the saturation magnetization value is 26.2 emu/g. Batch adsorption shows that the $Fe_3O_4$/PANI hollow spheres exhibit high uptake property of $Pb^{2+}$ in aqueous solution. The adsorption kinetics follows the mechanism of the pseudo-second-order kinetics and the sorption agrees well with Langmuir isotherm.

## Introduction

Due to the low density and high specific surface,[1-7] hollow spheres have attracted great research interests in waste removal, catalysis, and drug-release systems.[8-14] However, the main properties and performance can be altered or enhanced by introducing different shell materials. Especially, the hollow spheres whose shells combine two or more materials have received tremendous attention recently. Electromagnetic materials, as a unique class of bifunctional materials, have potential applications in electromagnetic shielding, microwave absorption, batteries and electrochemical display devices.[15-19]Among various available conductive polymers, polyaniline (PANI) has gained extensive interests because of its excellent environmental stability, low cost, and easy preparation. Recent researches have shown that polyaniline can be used as a potential sorbent for eliminating metal ions and dyes from aqueous solution.[20-23] However, the difficulties of removing and recycling particles limit its practical applications. Therefore, magnetic PANI composites, which can be recycled easily by external magnetic field, are expected to be an effective and eco-friendly sorbent.

Until now, a number of strategies have been developed to prepare PANI/$Fe_3O_4$ spheres. Deng et al.[24] fabricated PANI/$Fe_3O_4$ core/shell spheres via oxidative polymerization of aniline in an aqueous solution in the presence of surfactant dodecylbenzene sulfonic acid sodium salt and $Fe_3O_4$ particles. Xuan et al.[25] prepared $Fe_3O_4$/PANI core/shell spheres with blackberry-like morphology. In addition, the uniform hollow spheres may possess a lot of obvious advantages over the solid particles, which are versatile for many further developments.[26-29] It has potential applications in catalysis, lightweight fillers and encapsulation. Wang et al.[30] proposed a procedure by using conductive polyaniline as interior and $Fe_3O_4$ as exterior to prepare the electromagnetic hollow spheres against sulfonated polystyrene (PS) spheres as templates. Although this method is effective, PS spheres need to be sulfonated and PANI shell should be de-doped by ammonium hydroxide, which decreased the conductivity of the composite spheres. Xu et al.[31] also used sulfonated polystyrene as a template to obtain $Fe_3O_4$/PANI composite hollow spheres, and the conductivity was significantly enhanced after the template was modified by polyvinyl pyrrolidone (PVP). However, the saturated magnetization value of $Fe_3O_4$/PANI hollow spheres was low. Because the surfaces of PANI are hydrophobic while the $Fe_3O_4$ particles are hydrophilic, the synthesis of magnetic PANI spheres with both hollow and high saturated magnetization remains a big challenge.[32-34] Accordingly, it is significant to develop a moderate method to prepare hollow spheres with both PANI and magnetic particles as the shell.

Herein, we demonstrated a convenient method to prepare $Fe_3O_4$/PANI hollow composites by using PS spheres with positive charges as the hard templates. The synthetic process includes several steps: (1) preparation of monodisperse positive charged PS spheres via emulsion polymerization using 2,2'-azobisisobutyramidine dihydrochloride(AIBA) as cationic initiator, (2) adsorption of citric acid modified $Fe_3O_4$ particles onto the PS spheres, (3) coating PANI via in-situ oxidative polymerization as the outer shell, (4) removal of the PS core by dissolving with THF. The resultant $Fe_3O_4$/PANI hollow composites exhibit both conductivity and superparamagnetism.

Furthermore, the $Pb^{2+}$ removal properties of the $Fe_3O_4$/PANI adsorbents were evaluated in terms of the sorption kinetics and sorption isotherm.

## Experimental section

### Materials

Aniline (ANI) (AR grade, Shanghai Chemical Reagent Co.) and styrene (St) (AR grade, Tianjin Da Mao Chemical Reagent Co.) were distilled under reduced pressure before use. Ammonium persulfate (APS) (AR grade, Beijing Chem. Co.), polyvinyl pyrrolidone (PVP) (AR grade, Beijing Chem. Co.), citric acid (CA) (AR grade, Beijing Chem. Co.), 2,2'-azobisisobutyramidine dihydrochloride (AIBA) (AR grade, Beijing Chem. Co.) and $Fe_3O_4$ (Aladdin Chem. Co.) were used as received without further purification. Deionized water was used for all of the polymerization and treatment processes.

### Preparation of monodisperse PS spheres with positive charges

Monodisperse polystyrene spheres were prepared via emulsion polymerization using PVP and AIBA as emulsifier and cationic initiator, respectively. In a typical synthesis process, a mixture of 11 mL St, 1.5 g PVP and 140 mL water were added into a four-neck flask equipped with a condenser and a mechanical stirrer. After deoxygenation by bubbling $N_2$, the reaction mixture was heated up to 70 °C, and a solution of 0.26 g AIBA dissolved in 5 mL water was injected into the mixture. Then the reaction was allowed to proceed at 70 °C for 10 h. The resulting PS spheres were washed repeatedly with alcohol and water, followed by centrifugation, dried in a freeze drier for 24 h, and then stored in a desiccator for subsequent usage.

### Preparation of citric acid modified $Fe_3O_4$ nanoparticles

Citric acid modified $Fe_3O_4$ nanoparticles were prepared according to a typical procedure[35]: 2 g $Fe_3O_4$ nanoparticles were added into the solution of 8 g citric acid in 8 mL water and the reaction mixture was heated to 95°C under continuous stirring for 90 minutes.

### Preparation of PS/$Fe_3O_4$ spheres

A typical procedure for preparing PS/$Fe_3O_4$ spheres was to add 0.12 g citric acid modified $Fe_3O_4$ particles into 2.5 g PS emulsions. The reaction was performed under mechanical stirring for 30 min to obtain PS/$Fe_3O_4$ spheres.

### Preparation of PS/$Fe_3O_4$/PANI spheres and $Fe_3O_4$/PANI hollow spheres

A mixture of hydrochloric acid (2.5 M, 1 mL) and ANI (0.08 mL, the weight ratio of PS/PANI is 1:1.7) was added into the PS/ $Fe_3O_4$ suspension prepared above and stirred with a mechanical stirrer for 0.5 h in an ice/water bath. Then, APS (equimolar quantities with ANI) dissolved in water was added immediately to the dispersion with constant mechanical stirring. The reaction was carried out in an ice/water bath for 8 h and left it at room temperature for 16 h. The resultant products were washed repeatedly with alcohol until the filtrate became colorless. After the products were dried in a freeze drier for 24 h, the resultant PS/$Fe_3O_4$/PANI spheres were exposed to THF for 12 h to dissolve the PS and provided the $Fe_3O_4$/PANI hollow spheres.

### Adsorption experiments

Batch adsorption experiments were conducted to investigate the adsorption of $Pb^{2+}$ ions by $Fe_3O_4$/PANI hollow spheres. After adsorption, the sorbents were removed from the solution and the residual concentrations of $Pb^{2+}$ ions were measured by inductively coupled plasma atomic emission spectrometer (ICP-AES).

In order to evaluate kinetics, 0.01 g $Fe_3O_4$/PANI sorbents were added into 25 ml $Pb^{2+}$ aqueous solution with a concentration of 280 mg/L. Samples were taken at a desired period for the analysis of residual $Pb^{2+}$ concentration in solution.

Adsorption isotherm of $Pb^{2+}$ was carried out by adding 0.005g of the adsorbents into 25 mL of $Pb(NO_3)_2$ solution with $Pb^{2+}$ concentration ranging from 45 to 720 mg/L. After stirring the suspension for 4 h, the $Pb^{2+}$ concentration in the solution was analyzed. The amount of $Pb^{2+}$ ions adsorbed at equilibrium ($q_e$) was calculated according to the following equation (Eq.(1)), where $C_0$ and $C_e$ are initial and equilibrium concentrations of $Pb^{2+}$ ions, respectively, $m$ is the mass of adsorbent and $V$ is volume of the solution.

$$q_e = \frac{V(C_0 - C_e)}{m} \qquad (1)$$

### Characterization

A scanning electron microscopy (SEM, HITACHI S-4800) and a transmission electron microscopy (TEM, HITACHI H-800) were used to observe the morphology of the products. The infrared spectra were recorded by a Nicolet Avatar 360 FT-IR spectrophotometer using KBr disks. Vibrating sample magnetometer (Lake Shore 7410) was used to determine magnetic properties of the composite particles. X-ray diffraction (XRD, X' Pert PRO MPD) was used to determine the crystalline phase of materials.

## Results and discussion

As illustrated in Fig. 1, PANI hollow composite spheres are prepared by depositing $Fe_3O_4$ and PANI on positive PS spheres. The monodisperse positive PS spheres are prepared via emulsion polymerization by using PVP and AIBA as emulsifier and cationic initiator, respectively. Under continuous stirring, electronegative $Fe_3O_4$ particles, which are obtained by decorating $Fe_3O_4$ using citric acid,[36] are absorbed onto PS spheres to form "new templates" by virtue of the electrostatic interaction between the positively charged PS chains and the negatively charged $Fe_3O_4$.[37-39] What is more, the hydrogen bond interaction between the carboxyl groups of citric acid and PVP is another inevitable factor for $Fe_3O_4$ to be absorbed onto PS spheres.[40] Subsequently, the in-situ oxidative polymerization of aniline on the "new templates" is conducted. Eventually, $Fe_3O_4$/PANI hollow spheres are obtained via removing PS cores with THF. Images in Fig. 2 show the representative SEM and TEM pictures of the prepared PS spheres and composites. Based on SEM image shown in Fig. 2a, we can find that the average diameter of PS spheres is about 175 nm, and the size distribution is highly uniform. Fig. 2b

Cite this: DOI: 10.1039/c0xx00000x

www.rsc.org/xxxxxx

**ARTICLE TYPE**

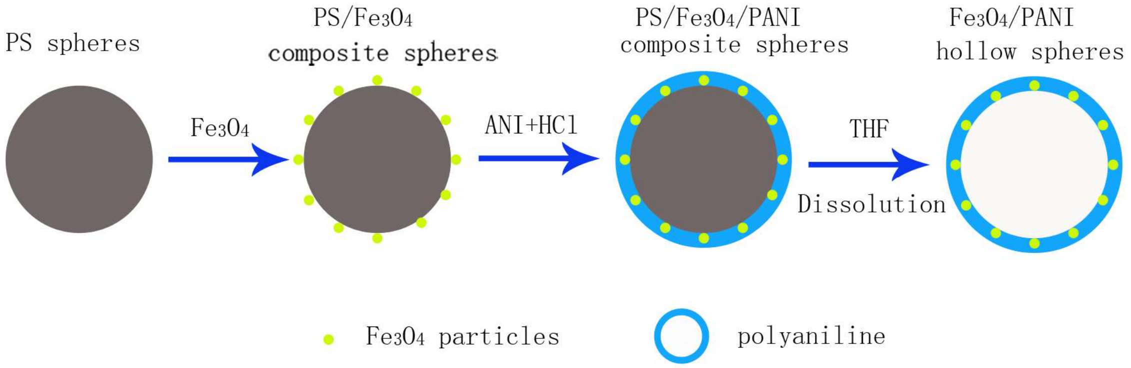

**Fig. 1** The preparation processes of $Fe_3O_4$/PANI hollow spheres

illustrates that $Fe_3O_4$ particles are deposited onto the surface of PS spheres, and the PS/$Fe_3O_4$ spheres are uniform, as the original PS template spheres. As shown in Fig. 2c, after the chemical oxidative polymerization of aniline, the surface of PS/$Fe_3O_4$/PANI spheres becomes rough as compared with that of original PS template spheres, and the sizes of PS/$Fe_3O_4$/PANI spheres enlarge. This indicates that PANI is coated on the PS/$Fe_3O_4$ spheres successfully. Furthermore, The hollow structure of resultant $Fe_3O_4$/PANI spheres is confirmed by TEM (Fig. 2d). One can clearly see from the TEM image that, after PS templates are removed, $Fe_3O_4$/PANI hollow spheres maintain the perfect spherical profile. Meanwhile, it is also apparent from the inset of Fig. 2d that the dark $Fe_3O_4$ particles embedded into the PANI shell do not be eroded, which demonstrates the successful achievement of electromagnetic hollow spheres.

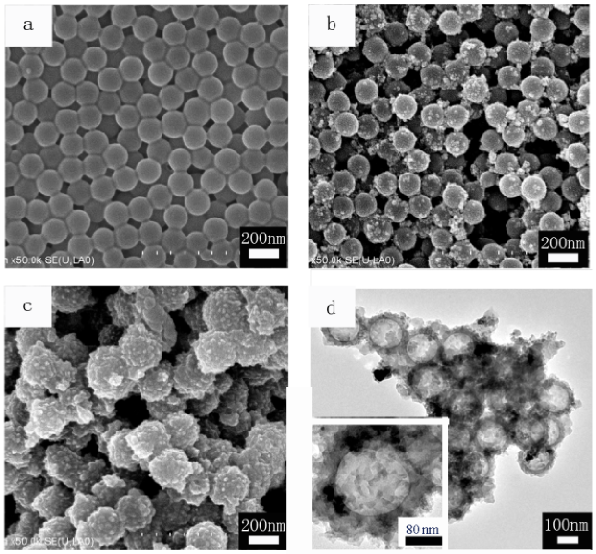

**Fig. 2** SEM images of (a) PS;(b) PS/$Fe_3O_4$; (c) PS/$Fe_3O_4$/PANI and TEM image of (d) $Fe_3O_4$/PANI hollow spheres (a typical high magnification image is shown in the inset)

FTIR spectroscopy was used to confirm the compositions of composite spheres. The spectra of PS spheres, PS/$Fe_3O_4$ spheres, PS/$Fe_3O_4$/PANI spheres and $Fe_3O_4$/PANI hollow spheres are shown in Fig. 3. The characteristic absorption peaks existed at 1496, 1457, 754, and 699 $cm^{-1}$correspond to the PS component (Fig. 3a,b,c). Except for the spectrum of PS (Fig. 3a), the band at 580 $cm^{-1}$ can be observed in other IR spectra, which is attributed to the Fe-O stretching vibration band of $Fe_3O_4$ particles.[41] Compared with the spectrum of PS/$Fe_3O_4$ spheres (Fig. 3b), the additional absorption bands in the spectrum of PS/$Fe_3O_4$/PANI spheres, which appear at 1305, 1247 and 1556 $cm^{-1}$, are ascribed to the PANI components (Fig. 3c). The bands at 1305 and 1247 $cm^{-1}$ are related to the C-N and C=N stretching modes, and the peak at 1556 $cm^{-1}$ is assigned to the quinone ring.[42] Most importantly, as indicted in Fig. 3d, the typical PS absorption bands (Fig.3a) are not found in the spectrum of $Fe_3O_4$/PANI hollow spheres, which indicates that the PS cores are fully removed. These results can be regarded as another powerful evidence for the formation of $Fe_3O_4$/PANI hollow spheres.

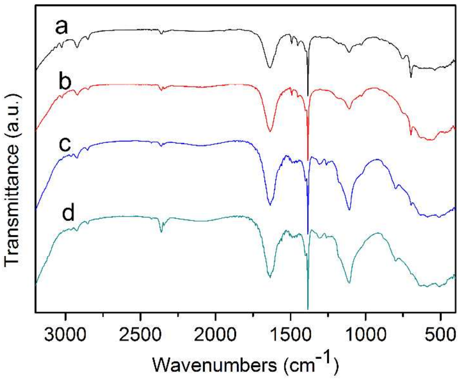

**Fig. 3** FTIR spectra of (a) PS spheres; (b) PS/$Fe_3O_4$ spheres; (c) PS/$Fe_3O_4$/PANI spheres and (d) $Fe_3O_4$/PANI hollow spheres

The existence of $Fe_3O_4$ particles and PANI shell can be further explored by X-ray diffraction (XRD). The XRD patterns of $Fe_3O_4$ particles, PS/$Fe_3O_4$/PANI spheres and $Fe_3O_4$/PANI hollow spheres are displayed in Fig.4. In the case of $Fe_3O_4$ particles (Fig. 4a), the characteristic peaks can be observed at $2\theta = 30.1°$, 35.2°, 43.3°, 53.5°, 57.3° and 62.5°, which are assigned to (2 2 0), (3 1 1), (4 0 0), (4 2 2), (5 1 1), and (4 4 0),[43] and they also appear in both Fig. 4b and 4c. Except for the $Fe_3O_4$ peaks, the broad part at the low scan angle of 25° shown in Fig. 4b and c could be ascribed to the amorphous polymer chains of PANI,[44] which reveals that PANI is successfully coated on the surface of PS/$Fe_3O_4$ templates. Moreover, Fig. 4c shows that $Fe_3O_4$ particles are existed in the PANI shell and also indicates that the crystal structure of $Fe_3O_4$ can be well maintained during the PANI polymerization process under the acidic condition. XRD results which also used to confirm the chemical compositions of composite spheres are consistent with the above FTIR analysis.

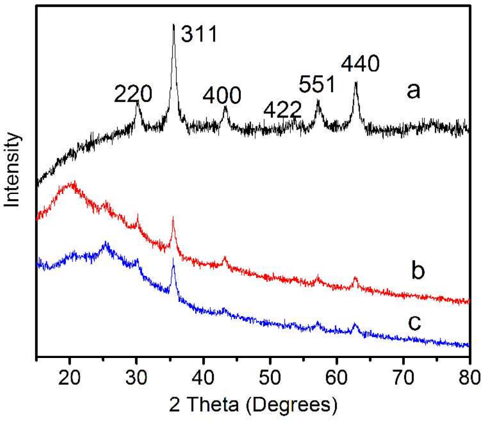

**Fig. 4**XRD patterns of (a) $Fe_3O_4$ particle; (b) PS/$Fe_3O_4$/PANI spheres; (c) $Fe_3O_4$/PANI hollow spheres

Vibrating sample magnetometer (VSM) was used to investigate the magnetic properties of the hollow composite spheres. The magnetization curve of the $Fe_3O_4$/PANI hollow composites is illustrated in Fig. 5a, and the saturation magnetization value is about 26.2 emu/g. Furthermore, neither remanence nor coercivityis observed in the magnetization curve, which indicates that the electromagnetic spheres possess superparamagnetic behavior.[45] As shown in Fig. 5b and c, the separation and recycling process of $Fe_3O_4$/PANI hollow composites is realized by external magnetic field, and the green $Fe_3O_4$/PANI composites dispersed in water (Fig. 5b) can be attracted toward the magnet in a short period (Fig. 5c). It can be used as a foundation for the further explore the magnetic separability, which may possess the potential applications in the water treatment processes.

To study how citric acid impacts the adsorption of $Fe_3O_4$ nanoparticles onto PS spheres, the $Fe_3O_4$ nanoparticles decorated by different amounts of citric acid were fabricated. Fig. 6 presents the SEM images of PS/$Fe_3O_4$ composite spheres, in which $Fe_3O_4$ particles are prepared at different weight ratios of citric acid and $Fe_3O_4$. When $Fe_3O_4$ particles are not decorated by citric acid, there are few $Fe_3O_4$ particles coated on the surface of PS spheres and the resultants are still smooth, as shown in Fig. 6a. The amount of $Fe_3O_4$ particles adsorbed onto PS spheres increase with increasing weight ratio of CA/$Fe_3O_4$ (Fig. 6b, c and d). This is because the $Fe_3O_4$ particles with high decoration degree introduce more COOH groups than that of low decoration degree, which will favor more $Fe_3O_4$ nanoparticles to be coated on PS spheres, due to the stronger electrostatic interaction between the positively charged PS spheres and the negatively charged $Fe_3O_4$. Simultaneously, more COOH groups on the surface of $Fe_3O_4$ nanoparticlescan provide more sites to form hydrogen bond between COOH group and PVP. Consequently, citric acid plays an important role of successful coating of $Fe_3O_4$ nanoparticles onto positive PS spheres.

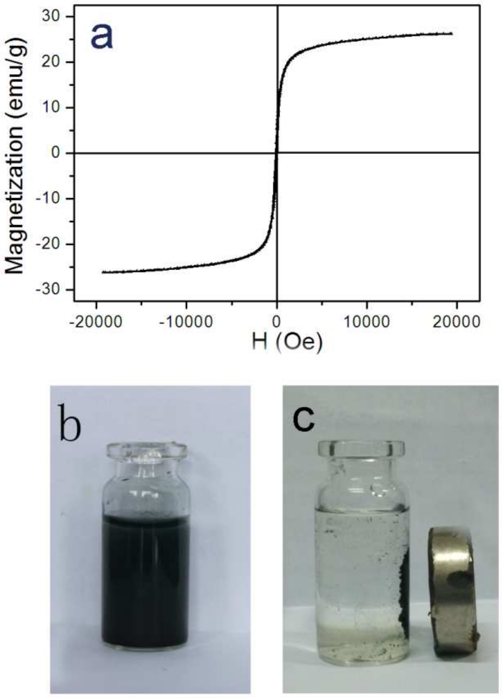

**Fig. 5** Magnetization curve of $Fe_3O_4$/PANI hollow spheres measured at room temperature (a); the photographs of $Fe_3O_4$/PANI hollow spheres dispersed in water (b) and separability by external magnetic field (c)

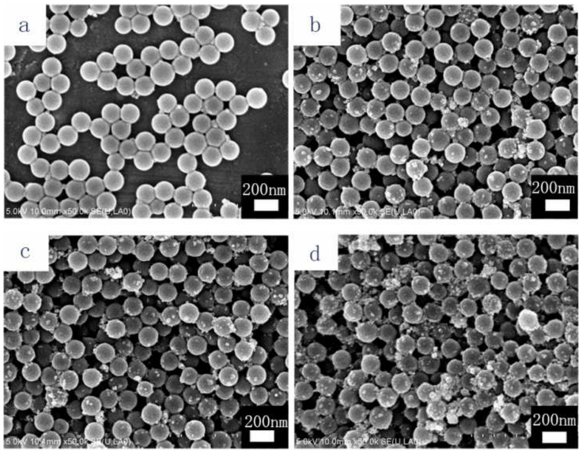

**Fig. 6** SEM images of PS/$Fe_3O_4$ spheres prepared with different weight ratios of citric acid and $Fe_3O_4$: (a) 0:1; (b) 0.1:1; (c) 1:1; (d) 10:1

Because of the presence of amine and imine functional groups, PANI can chelate with some heavy-metal ions taking advantage of affinity of nitrogen.[46] The influence of adsorption time on the removal of $Pb^{2+}$ by $Fe_3O_4$/PANI hollow spheres is shown in Fig. 7, which depicts the temporal evolution of $Pb^{2+}$adsorption capacity and the adsorption kinetics by $Fe_3O_4$/PANI. At the initial stage, the adsorption capacity increases dramatically, with prolonged adsorption time, the increment becomes slower. After 60 min, the adsorption reaches the saturation level, meaning chelating with heavy-metal ions $Pb^{2+}$ by the PANI reaches equilibrium.

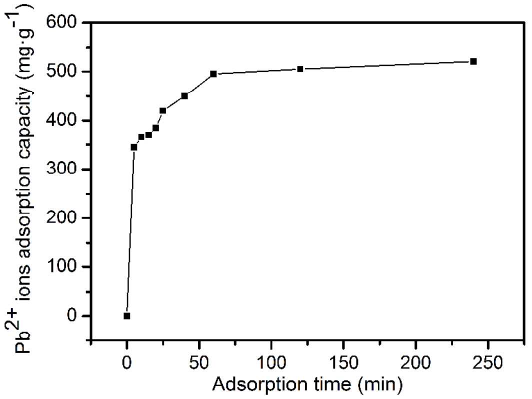

**Fig. 7** Effect of adsorption time on the removal of $Pb^{2+}$ by $Fe_3O_4$/PANI hollow spheres

In order to evaluate the adsorption mechanism of $Pb^{2+}$ onto the $Fe_3O_4$/PANI, pseudo-first-order (Eq.(2)) and pseudo-second-order models (Eq.(3)) were used to interpret the experimental data, where $q_e$ (mg/g) and $q_t$ (mg/g) denote the uptake capacity of $Pb^{2+}$ corresponding to the equilibrium time and a set time t, respectively, while $k_1$ and $h$ are the rate constant of pseudo-first-order and the initial adsorption rate of pseudo-second-order, respectively.

$$\ln(q_e - q_t) = \ln q_e - K_1 t \quad (2)$$

$$\frac{t}{q_t} = \frac{1}{h} + \frac{t}{q_e} \quad (3)$$

The corresponding kinetic parameters and the correlation coefficient are shown in Table 1. The good correlation coefficient displayed in Table 1 implies that the adsorption kinetic of $Pb^{2+}$ ions onto $Fe_3O_4$/PANI sorbents can be described better by the pseudo-second-order mode rather than pseudo-first-order. The experimental adsorption capacity $q_e$ value can reach as high as 535 mg/g (Fig. 7), which is in agreement with the calculated number (531 mg/g, Table 1), suggesting that the adsorption mechanism is chemisorption. Consequently, it infers that the adsorption process is mainly controlled by the chemical complexation between metal ions and binding sites.[47] Furthermore, both increase of the thickness of PANI shell and decrease of the amount of $Fe_3O_4$ nanoparticles can enhance the adsorption capacities for $Pb^{2+}$ by $Fe_3O_4$/PANI adsorbents (Table S1, Table S2 in Supporting Information). These results suggest that the potential applications in the water treatment processes.

**Table 1** Kinetic parameters for $Pb^{2+}$ ions adsorption onto hollow $Fe_3O_4$/PANI spheres

| Mathematical mode | $R^2$ | Rate constant | $q_m$ (mg·g$^{-1}$) |
|---|---|---|---|
| Pseudo-first-order | 0.8313 | 0.026 min$^{-1}$ | 228.7 |
| Pseudo-second-order | 0.9995 | 93 mg·g·min$^{-1}$ | 531.9 |

Two mathematical models, Freundlich and Langmuir isotherm, were adopted to analyze isotherm data. Freundlich (Eq. (4)) and Langmuir (Eq. (5)) equations can be expressed as follows:

$$\log q_e = \log K_F + \frac{1}{n \log C_e} \quad (4)$$

$$\frac{C_e}{q_e} = \frac{1}{K_L} + \frac{C_e}{q_m} \quad (5)$$

Where $q_m$ (mg/g) is theoretical maximum adsorption capacity of the adsorbent for $Pb^{2+}$, $K_F$ and n are Freundlich empirical constants, and $K_L$ (L/mg) is Langmuir binding constant related to the energy of adsorption.

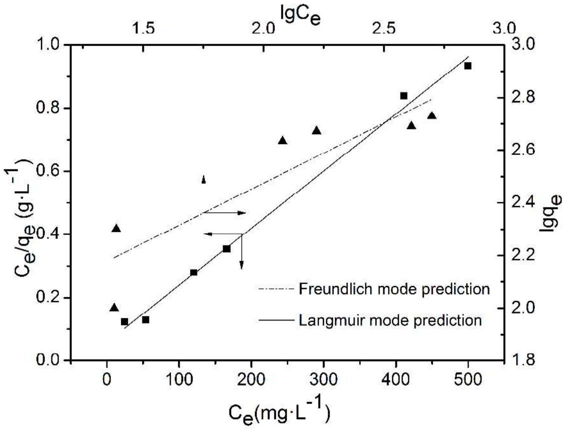

**Fig. 8** Freundlich and Langmuir plots of the adsorption of $Pb^{2+}$ onto $Fe_3O_4$/PANI in concentration ranging from 45 to 720 mg/L

**Table 2** Parameters for $Pb^{2+}$ ions adsorption onto hollow $Fe_3O_4$/PANI spheres according to Langmuir and Freundlich equilibrium models

| Langmuir | | | Freundlich | | |
|---|---|---|---|---|---|
| $R^2$ | $Q_m$ ( mg·g$^{-1}$) | $K_L$ (L ·mg$^{-1}$) | $R^2$ | n | $K_f$ |
| 0.9934 | 552 | 0.031 | 0.7627 | 2.19 | 36.31 |

The Freundlich and Langmuir plots of the adsorption of $Pb^{2+}$ by $Fe_3O_4$/PANI sorbents are illustrated in Fig. 8 as function of the concentration of $Pb^{2+}$. The related Freundlich and Langmuir constants were measured, and the results are presented in Table 2. As indicated in Table 2, according to the calculated correction coefficients, the adsorption isotherm behavior of $Pb^{2+}$ onto $Fe_3O_4$/PANI sorbents can be described better by the Langmuir isotherm rather than Freundlich isotherm. These results imply that the binding sites are homogeneous with equivalent sorption energies on the surface of adsorbent.[48,49]

## Conclusions

In this work, monodisperse electromagnetic $Fe_3O_4$/PANI hollow spheres, possessing high adsorption capacity toward $Pb^{2+}$, were constructed by deposition $Fe_3O_4$ and PANI on PS spheres. In the synthetic process, citric acid plays an important role of successful coating of $Fe_3O_4$ nanoparticles onto PS. The hydrogen bond interaction between the carboxyl groups of citric acid and PVP, and the electrostatic interaction between the positively charged PS chains and the negatively charged $Fe_3O_4$ decorated by citric acid are two crucial factors for $Fe_3O_4$to be absorbed onto PS spheres. $Fe_3O_4$ nanoparticles are embedded into the PANI shell. The electromagnetic composites exhibit a superparamagnetic behavior with saturation magnetization value about 26.2 emu/g, and the composite spheres can be separated from solution under an external magnetic field. Moreover, the adsorption experiments of the obtained magnetic PANI hollow spheres toward $Pb^{2+}$ show that the adsorption capacity can reach up to 535 mg/g and the adsorption kinetics and the sorption follow the mechanism of the pseudo-second-order equation and Langmuir isotherm respectively, and the adsorption capacity is affected by the thickness of PANI shell and the amount of $Fe_3O_4$. Considering the excellent adsorption capacity and recycling ability, the $Fe_3O_4$/PANI hollow spheres is a potential sorbent of wide applicability to remove heavy metals from water.

## Acknowledgments

Financial support from the National Science Foundation of China (no. 50873017 and 51374219) is gratefully acknowledged.

## Notes and references

*[a]Beijing Key Laboratory of Energy Conversion and Storage Materials, College of Chemistry,Beijing Normal University, Beijing 100875, China*
*E-mail: hly@bnu.edu.cn*
*[b] Enhanced Oil Recovery Research Institute, China University of Petroleum, Beijing 102249, China*

† Electronic supplementary information (ESI) available: Adsorption capacities for $Pb^{2+}$ by $Fe_3O_4$/PANI adsorbents prepared with different weigh ratio of ANI/PS and various amount of citric acid modified $Fe_3O_4$ particles. See DOI: 10.1039 / ×××××××.

1 F. Caruso, R. A. Caruso and H. Möhwald, *Science*, 1998, **282**, 1111-1114.
2 J. Hu, M. Chen, X. Fang, L. Wu, *Chem. Soc. Rev*, 2011, **40**, 5472－5491.
3 M. Yang, J. Ma, C. Zhang, Z. Yang and Y. Lu, *Angew. Chem., Int. Ed.*, 2005, **44**, 6727-6730.
4 J. Hu, M. Chen and L. Wu, *Polym. Chem.*, 2011, **2**, 760-772.
5 M. Ji, H. Liu and X. Yang, *Polym. Chem*, 2011, **2**, 148-156.
6 M. Yang, J. Ma, Z. Niu, X. Dong, H. Xu, Z. Meng, Z. Jin, Y. Lu, Z. Hu and Z. Yang, *Adv. Funct. Mater.*, 2005, **15**, 1523-1528.
7 T. Chen T, P. Colver, S. Bon, *Adv. Mater.*, 2007, **19**, 2286-2289.
8 X. Yang, L. Chen, B. Huang, F. Bai, X. Yang, *Polymer*, 2009, **50**, 3556-3563.
9 H. Ding, G. Wang, M. Yang, Y. Luan, Y. Wang and X. Yao, *J Mol Catal a-Chem*, 2009, **308**, 25-31.
10 S. Xuan, F. Wang, J. M. Y. Lai, K. W. Y. Sham, Y.-X. J. Wang, S.-F. Lee, J. C. Yu, C. H. K. Cheng and K. C.-F. Leung, *ACS Appl Mater Inter* , 2011, **3**, 237-244.
11 J. Yang, J. Lee, J. Kang, K. Lee, J.-S. Suh, H.-G. Yoon, Y.-M. Huh and S. Haam, *Langmuir*, 2008, **24**, 3417-3421.
12 X. Yang, L. Chen, B. Han, X. Yang and H. Duan, *Polymer*, 2010, **51**, 2533-2539.
13 M. Chen, L. Wu, S. Zhou and B. You, *Adv. Mater.*, 2006,**18**, 801-806.
14 Z. Wang, L. Wu, M. Chen and S. Zhou, *J. Am. Chem. Soc.*, 2009, **131**, 11276-11277.
15 T. Yao, T. Cui, J. Wu, Q. Chen, S. Lu and K. Sun,*Polym. Chem.*, 2011, **2**, 2893-2899.
16 P. Saini, V. Choudhary, N. Vijayan and R. K. Kotnala, *J. Phys. Chem. C*, 2012, **116**, 13403-13412.
17 S. Xuan, Y.-X. J. Wang, J. C. Yu and K. C.-F. Leung, *Langmuir*, 2009, **25**, 11835-11843.
18 Y. L. Yang, M. C. Gupta, *NanoLett.*, 2005, **5**, 2131－2134.
19 K. Singh, A. Ohlan, P. Saini and S. K. Dhawan, *Polym. Advan. Technol.*, 2008, **19**, 229-236.
20 N. Jiang, Y. Xu, Y. Dai, W. Luo and L. Dai, *J. Hazard Mater.*, 2012, **215－216**, 17-24.
21 D. Mahanta, G. Madras, S. Radhakrishnan, S. Patil, *J. Phys. Chem. B*, 2008, **112**, 10153-10157.
22 D. Mahanta, G. Madras, S. Radhakrishnan, *J. Phys. Chem. B*, 2009, **113**, 2293-2299.
23 X. Huang, G. Wang, M. Yang, W. Guo and H. Gao, *Mater. Lett.*, 2011, **65**, 2887-2890.
24 J. Deng, C. He, Y. Peng, J. Wang, X. Long, P. Li , *Synth. Met.*, 2003, **139**, 295-301.
25 S. Xuan, Y.-X. J. Wang, K. C.-F. Leung and K. Shu, *J. Phys. Chem. C*, 2008, **112**, 18804-18809.
26 J. Han, J. Dai and R. Guo, *J. Colloid. Interf. Sci.*, 2011, **356**, 749-756.
27 Y. Yin, M. Chen, S. Zhou, L. Wu, *J. Mater. Chem.*, 2012, **22**, 11245-11251.
28 D. Yu, X. Sun, J. Zou, Z. Wang, F. Wang, K. Tang, *J. Phys. Chem. B*, 2006, **110**, 21667-21671.
29 Y. Cao, B. You, L. Wu , *Langmuir*, 2010, **26**, 6115-6118.
30 X. Wang, S. Tang, J. Liu, Z. He, L. An, C. Zhang, J. Hao, W. Feng, *J. Nanopart. Res.*, 2009, **11**, 923-929.
31 H. Xu, H. Zhang, T. Lv, H. Wei, F. Song, *Colloid. Polym. Sci.*, 2013, **291**, 1713-1720.
32 H. Wang, R. Wang, L. Wang and X. Tian, *Colliod Surface A* , 2011, **384**, 624-629.
33 B. Liu, W. Zhang, F. Yang, H. Feng and X. Yang, *J. Phys. Chem. C*, 2011, **115**, 15875-15884.
34 G. Liu, H. Wang and X. Yang, *Polymer*, 2009, **50**, 2578-2586.
35 Y. Han, D. Radziuk, D. Shchukin, H. Moehwald, *Macromol. Rapid Comm.*, 2008, **29**, 1203-1207.
36 Y. Sahoo, A. Goodarzi, M. T. Swihart, T. Y. Ohulchanskyy, N. Kaur, E. P. Furlani, P. N. Prasad, *J. Phys. Chem. B*, 2005, **109**,3879-3885.
37 Y. Li, Z. Wang, Q. Wang, C. Wang, G. Xue, *Macromolecules*, 2010, **43**, 4468-4471.
38 M. Chen, S. Zhou, B. You and L. Wu, *Macromolecules*, 2005, **38**, 6411-6417.
39 J. Yuan, S. Zhou, B. You and L. Wu, *Chem. Mater*, 2005, **17**, 3587-3594.
40 W. Leng, M. Chen, S. Zhou and L. Wu, *Langmuir*, 2010, **26**, 14271-14275.
41 L. Zhang, T. Wang, P. Liu, *Chem. Eng. J.*, 2012, **187**, 372-379.
42 L. Wang, H. Liang, F. Wang, L. Huang, Z. Liu and Z. Dong, *Langmuir*, 2013, **29**, 5863-5868.
43 D. A. Marsh, M. W. Szyndler, R. M. Corn and A. S. Borovik, *Polym. Chem.*, 2012, **3**, 2852-2856.
44 R. M. Khafagy, *J. Alloy Compd.*, 2011, **509**, 9849-9857.
45 W. He, L. Cheng, L. Zhang, Z. Liu, Z. Cheng and X. Zhu, *Polym. Chem.*, 2014, **5**, 638-645.
46 J. Han, P. Fang, J. Dai, R. Guo, *Langmuir*, 2012, **28**, 6468-6475.
47 Y. S. Ho and G. McKay, *Process Biochem.*, 1999, **34**, 451-465.
48 S. Al-Asheh, F. Banat, R. Al-Omari and Z. Duvnjak, *Chemosphere*, 2000, **41**, 659-665.
49 D. Mahanta, N. Munichandraiah, S. Radhakrishnan, G. Madras and S. Patil,*Synth. Met., 2011,* ***161****, 659-664.*